RSC Advances

PAPER

View Article Online
View Journal | View Issue

Cite this: *RSC Adv.*, 2016, **6**, 97921

2,2′:6′,2″-Terpyridine-functionalized redox-responsive hydrogels as a platform for multi responsive amphiphilic polymer membranes†

Katrin Schöller,‡[a] Claudio Toncelli,‡[a] Juliette Experton,[a] Susanne Widmer,[a] Daniel Rentsch,[b] Aliaksei Vetushka,[c] Colin J. Martin,[d] Manfred Heuberger,[a] Catherine. E. Housecroft,[d] Edwin C. Constable,[d] Luciano F. Boesel*[a] and Lukas J. Scherer[a]

Nanophase-separated amphiphilic polymer co-networks are ideally suited as responsive membranes due to their stable co-continuous structure. Their functionalization with redox-responsive 2,2′:6′,2″-terpyridine–metal complexes and light-responsive spiropyran derivatives leads to a novel material with tunable optical, redox and permeability properties. The versatility of the system in complexing various metal ions, such as cobalt or iron at different concentrations, results in a perfect monitoring over the degree of crosslinking of the hydrophilic poly(2-hydroxyethyl acrylate) channels. The reversibility of the complexation, the redox state of the metal and the isomerization to the merocyanine form upon UV illumination was evidenced by cyclic voltammetry, UV-Vis and permeability measurements under sequential conditions. Thus, the membrane provides light and redox addressable functionalities due to its adjustable and mechanically stable hydrogel network.

Received 23rd September 2016
Accepted 7th October 2016

DOI: 10.1039/c6ra23677d

www.rsc.org/advances

Introduction

Amphiphilic co-networks (APCNs) have been drawing the interest of scientists from different fields due to their peculiar polymer platform which consists of interconnected hydrophilic/hydrophobic phases of co-continuous morphology.[1] APCNs are able to swell and form gel structures both in water and organic phases.[2] The versatility of the synthesis approach and the variety of functional monomers, bi and poly-functional cross-linkers allows fine tuning of the overall network properties with phase separation occurring even at the nanoscale.[3] The modulation of such properties allows the targeting of defined swelling in aqueous and organic solvents, permeability of gas and host molecules as well as entrapment and localized diffusion of host molecules in targeted areas.[1] Hence, these co-networks are generally employed in the synthesis of drug-delivery systems,[4] scaffolds for tissue engineering,[5] biocatalysts and nanoreactors,[6] contact lenses,[7] biosensors[8] and body implants.[9]

In particular, application in tissue engineering and drug delivery not only aim at the above mentioned properties, but it is also desirable to change these properties in response to an external stimulus. Thus, the host matrix may itself control and tune the features of such "smart" materials through local shifts in pH, ionic strength, temperature or oxidant level.[10] In addition, in the case of drug-delivery nanocarriers, external stimuli such as magnetic, light, ultrasonic and electric fields could be utilized for remote switching of network hydrophilicity, local heat control and guidance of the drug content in the targeted area.[11] The stimuli not only serve to selectively release the drug content in the designated area, but it might alter the pharmacokinetics in order to attain a linear diffusion and therefore prolong the controlled release rate for a spatial, temporal as well as dose control precision.[12]

Dual and multi-stimuli responsiveness have been actively investigated in an effort to further improve the precision of the response and enhance the switching window.[13]

Light-responsive materials have been used to remotely trigger the hydrogel hydrophilicity *via* immobilization of azobenzene,[14] stilbene,[15] diarylethene,[16] fulgides[17] and spiropyrans. The latter has been widely studied due to the range of stimuli able to induce its reversible isomerization, which, besides light, also includes different solvents, metal ions, acids and bases, temperature, redox potential, and mechanical force.[18–22]

[a]*Empa, Swiss Federal Laboratories for Materials Science and Technology, Lerchenfeldstrasse 5, 9014 St. Gallen, Switzerland. E-mail: luciano.boesel@empa.ch*

[b]*Empa, Swiss Federal Laboratories for Materials Science and Technology, Überlandstrasse 129, 8600 Dübendorf, Switzerland*

[c]*Laboratory of Nanostructures and Nanomaterials, Institute of Physics AS CR, Cukrovarnicka 10, 162 00 Prague 6, Czech Republic*

[d]*Department of Chemistry, University of Basel, Spitalstrasse 51, 4056 Basel, Switzerland*

† Electronic supplementary information (ESI) available. See DOI: 10.1039/c6ra23677d

‡ These authors contributed equally.

Redox sensitive polymeric carriers are appealing for triggered drug delivery as cytosol and cell nuclei contain 4–400 times higher concentration of reducing glutathione (GSH) tripeptide relative to body fluids (0.5–10 mM *versus* 2–20 mM GSH).[23] Moreover, *in vivo* research has demonstrated that in mice 4-fold higher GSH concentrations are present in tumor tissues compared to non-carcinogenic ones.[24]

On the other hand, oxidation-responsive nanocarriers might liberate their payload when elevated levels of reactive oxygen species, including superoxide, hydrogen peroxide, and hydroxide radicals, are present, since such levels are often observed in cellular inflammation as part of the non-specific immune reaction.[25]

In the last decade, metal-induced cross-linking has become a promising alternative to the more popular redox responsive materials bearing di-sulfide or di-selenide linkages.[26] Indeed, metallo-supramolecular polymers not only exhibited structural integrity in aqueous solution under different conditions (pH and temperature), but provide the possibility of precisely controlled release profiles of their encapsulated hydrophobic guest molecules *via* the combination of varying stimuli.[27]

Although ferrocenyl moieties are the most investigated metal–organic frameworks (MOFs), the exclusive motif of Fe(II)/Fe(III) redox couple does not suffice for a fine-tuning of the permeability and swelling properties.[28] Benzimidazole moieties,[29] carboxylic moieties in benzene tricarboxylic ligands[30] or poly(acrylic acids)[31] and amino groups in chitosan[32] offer a wider range of metal ion redox switches that can be utilized for such purposes. However, these mono-dentate ligands are often characterized by a weak coordinating bond, which might hamper the gel stability outside the target delivery area. Pyridine ligands, such as pyridine,[33] 2,2′-bipyridine[34] and 2,2′:6′,2″-terpyridine[35] (tpy) offer remarkably stable metal complexes. In particular, one of the first redox switches for biomedical applications employed the redox couple Ru(II)/Ru(III) in the presence of tpy.[36]

However, as demonstrated by Meier *et al.*,[37] other metal ions could be employed for MOFs assembly, with the relative binding strength (*i.e.* related to the metal-induced cross-linked network stability) following this sequence: Co > Ru > Fe > Ni > Cu > Mn > Cd.

In the case of the Co(II)/Co(III)[38,39] and Fe(II)/Fe(III)[40] couples, the redox change has proved to impart different optical, mechanical and swelling/permeability properties.

In this paper, a dual responsive system based on spiropyran and terpyridine ligands is hereby synthesized by covalent immobilization on APCN co-network membrane constituted of poly((trimethylsilyl)oxyethylmethacrylate) (poly(TMS-HEA)) and a poly(dimethylsiloxane) dimethacrylate (PDMS-DMA) as cross-linker.

The optical and mechanical behavior during switching from non-complexed to complexed state in the presence of Co(II) metal ions was characterized by UV-Vis measurements and atomic force microscopy (AFM). De-complexation was attained by the competitive ligation of Co(II) with hydroxyethyl(ethylenediaminetriacetic acid) (HEEDTA) (Scheme 1).

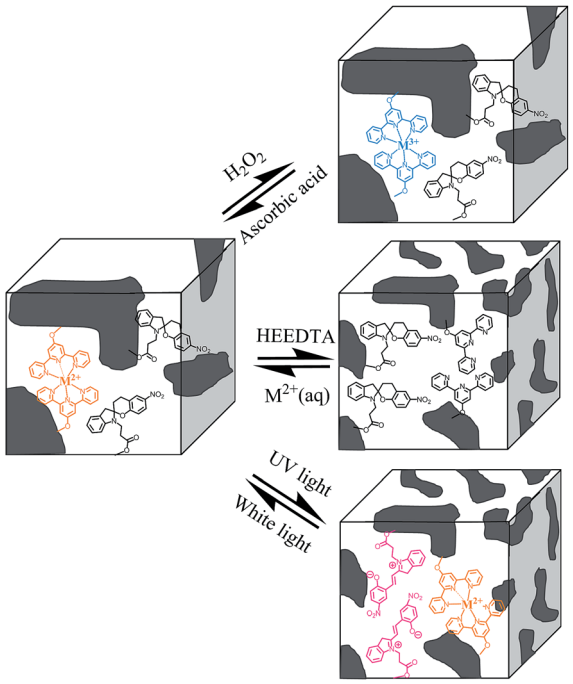

Scheme 1 Possible responses of multi stimuli-responsive membranes from 2,2′:6′,2″-terpyridine (TP1) and spiropyran side-chain functionalized amphiphilic polymer networks (orange colour: M^{2+}/TP1 complex, blue colour: M^{3+}/TP1 complex, pink colour: spiropyran in the merocyanine form).

The different complexation/de-complexation and redox states combined with the light switch induced by the presence of spiropyran moieties in the APCNs were evaluated on the basis of their morphological, optical and redox properties.

Experimental section

Materials

Microscope glass slides from Thermo Scientific were used as support and cover for the membrane production. Self-adhesive tape (Tesafilm universal, transparent) was used as spacer unit between the two glass slides. 2-((Trimethylsilyl)oxy)ethyl acrylate (TMS-HEA) and α,ω-methacryloxypropyl poly(dimethylsiloxane) (PDMS-DMA), (48 to 75 monomer units) were purchased from ABCR. TMS-HEA, acryloyl chloride (Sigma-Aldrich) and 2-hydroxyethylacrylate (Sigma-Aldrich) were distilled under reduced pressure before usage and stored in the freezer for no more than one month. Irgacure 819 was provided by BASF.

Bromine, 2,3,3-trimethylindolenine, 3-iodopropionic acid, 4-dimethylaminopyridine, *N*,*N*′-dicyclohexylcarbodiimide, 4′-chloro-2,2′:6′,2″-terpyridine, piperidine, 2-hydroxy-5-nitrobenzaldehyde, trimethylamine, 1,6-hexandiol, hydrogen peroxide 30 wt% in water, 2-butanone, L-ascorbic acid, iron(II) and cobalt(II) chloride tetrahydrates were purchased from Sigma-Aldrich.

Hexane was purchased from Biosolve. Tetrahydrofuran (THF), dimethylsulfoxide (DMSO), toluene, methanol and dichloromethane were purchased from Fisher Chemicals. Dichloromethane extra-dry and magnesium sulfate were purchased by Acros Organics. Caffeine and potassium

carbonate anhydrous and potassium hydroxide in pellets were purchased from Fluka. Trilon D liquid, an aqueous solution of hydroxyethyl(ethylenediaminetriacetic acid) (HEEDTA) (39.0–41.0 wt%) was kindly provided by BASF. Unless stated otherwise, all chemicals were used as purchased without further purification and distilled water from the in-house supply was used.

Preparation of monomer solutions

Spirobenzopyran covalently immobilized on an acrylate moiety (SP) (Scheme 2) was synthesized as reported earlier by our group[20] (36% yield). The tpy ligand directly anchored to an acrylate moiety *via* an aliphatic spacer (Scheme 2) was synthesized according to literature in 49% overall yield.[41] Detailed descriptions of analytical characterization of the reactants can be found in the ESI.†

Complexation/de-complexation studies of TP1

UV-Vis spectra of solutions and membranes (in the switching studies) were performed on a Biotek Synergy Mx microplate reader. The characterization of monomers in solution after multiple oxidation/reduction cycles was performed with 4 solutions each containing 1.83 mg TP1 and 0.44 mg $CoCl_2 \cdot 4H_2O$ in 1.1 mL of methanol. In the first solution, UV-Vis was measured without any further treatment. Each of the four solutions were used to characterize two consecutive redox cycles: (i) original Co(II)/TP1 complex, (ii) formation of Co(III)/TP1 complex by oxidation with bromine for 3 min, (iii) reduction to yield back the Co(II)/TP1 complex by adding 40 mg of ascorbic acid and (iv) second oxidation to synthesize Co(III)/TP1.

Synthesis of functionalized APCNs

Three different weight ratios (50/50, 60/40, and 70/30 wt%, written as 50/50, 60/40, and 70/30 in the text) of TMS-HEA to PDMS-DMA were used to produce membranes. If not stated otherwise, 60/40 membranes were used. The thickness of the membrane was adjusted by the number of tesa film stripes which were piled on each other as spacers. Each stripe was about 50 μm thick (*e.g.* for a spacer built of four layers tape, membranes with a thickness of 200 μm were produced). In total, 0.625 g of monomer and cross-linker mixture was used per membrane. After premixing of TMS-HEA with TP1 (from 1.25 mg, 0.0031 mmol to 20 mg, 0.050 mmol) and/or SP (6.25 mg, 0.013 mmol), Irgacure 819 (5 mg, 0.01 mmol) were added under red light and the mixture was shaken vigorously for 3 min. Thereafter, the corresponding amount of PDMS-DMA was added and the mixture shaken again for 1 min (Scheme 3).

The formulations were inserted as liquid precursors between two glass slides and irradiated for 20 min with white light (500 W lamp). Subsequently, the slides were placed into a mixture of THF and water (50/50 vol%) in order to minimize the adhesion between the synthesized APCNs and the glass slides. After 12 h, the membrane was removed and stored in distilled water to avoid the complete drying of the membrane.

Complexation/de-complexation studies

To ensure the maximum chelation of available terpyridine sites in the membranes with the metal ions (*i.e.* Co(II), Fe(II)), the APCNs were immersed in an aqueous solution of 10 g L^{-1} $FeCl_2 \cdot 4H_2O$ or $CoCl_2 \cdot 4H_2O$ for 2 days, unless stated otherwise.

Subsequently, the membranes were rinsed thoroughly with water to remove excess metal ions. De-complexation was performed by immersing the APCNs in an aqueous solution of 40 wt% HEEDTA for 5 h.

Six membranes were immersed for 1 min in six different solutions of iron and cobalt chloride at concentrations of 1 g L^{-1}, 5 g L^{-1} and 10 g L^{-1}.

After drying in a desiccator over molecular sieves for 18 h, their UV-Vis spectra were recorded. The experiment was repeated with the same membranes after total complexation times of 10 min, 30 min, 1 h, 2 h, 4 h, 8 h, 12 h, 16 h, 24 h, 32 h and 48 h.

Oxido-reduction cycles of Co(II)/Co(III) terpyridyl complex

Co(II) complexed APCNs were oxidized to Co(III) complex in an aqueous solution of 30 vol% hydrogen peroxide for 2 h (in case

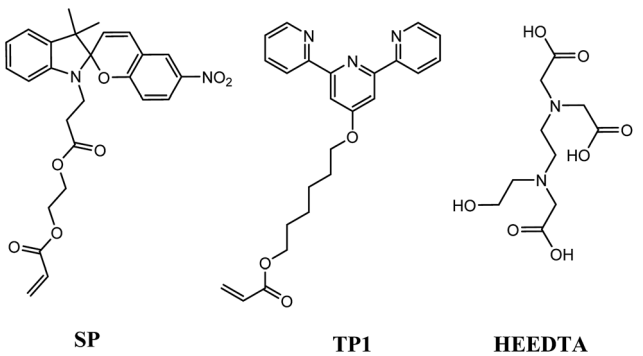

Scheme 2 Structures of the SP and TP1 monomers employed in the preparation of multi-stimuli-responsive APCNs and the employed de-complexing agent (HEEDTA).

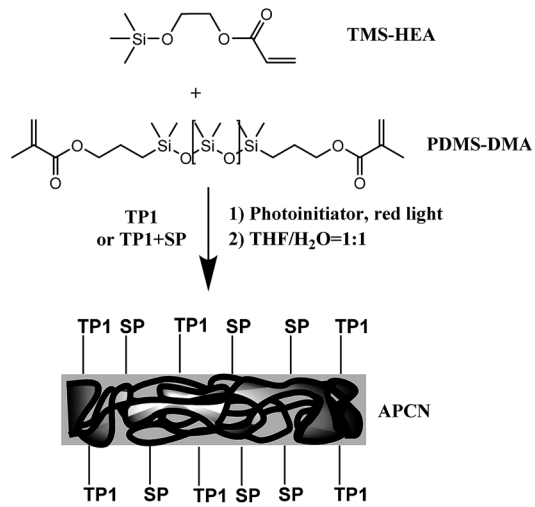

Scheme 3 Synthesis of APCNs functionalized with TP1 and SP.

only the monomer solution was tested, H_2O_2 was not strong enough for oxidation, thus bromine vapour was employed[42]) followed by rinsing the APCNs with water. To reduce the Co(III) to Co(II) in the second cycle, a 100 g L^{-1} solution of ascorbic acid in water was applied for 1 h.

Characterization

Solid-state UV measurements of complexation kinetics were performed using a Lambda 9 spectrometer (Perkin Elmer) in transmission mode.

Peak Force Quantitative Mechanical Property Mapping at the Nanoscale (Peak Force QNM) were performed on a Bruker Icon Atomic Force Microscope (AFM) using silicon Nanoscience Aspire CFMR cantilevers with a force constant of 3 N m^{-1}, and a resonant frequency of 75 kHz. The radius of a new tip was ±8 nm. The set point of the peak force applied during the measurements was 1 nN, the peak force frequency was 2 kHz. The cantilever was calibrated on a Bruker PDMS-SOFT-2-12M test sample (nominal elastic modulus was 3.5 MPa). The scanning speed was 250 nm s^{-1}. All AFM measurements were performed at 25 °C and approx. 30% humidity of the ambient air.

In order to calculate the membrane swelling, all dimensions were callipered with a Mitutoyo 522 Diamond Master Vernier. A membrane was dried in the desiccator over 4 Å molecular sieves for one day. Afterwards, its volume (V_0) was determined by measuring the side lengths and the thickness. Then the membrane was placed into water or hexane for 24 h and the volume (V_1) was measured again. For measuring the impact of the merocyanine state on the swelling behavior, a membrane was illuminated with UV-light (366 nm, 8 mW cm^{-2}) during the entire measurement. Each measurement was repeated three times. The volumetric degree of swelling S was calculated using the following formula:

$$S = V_1/V_0 \quad (1)$$

The water contact angles of the membranes were determined with a Krüss Contact angle DSA25 device. The membranes were previously dried in a desiccator over molecular sieves for 18 h.

The value given is an average over 10 measurements at different spots per sample.

All permeability measurements were performed in a Franz diffusion-cell (SES Analysis system, receptor volume 12.0 mL and orifice area 1.77 cm^2). Before placing the membranes in the Franz cell, they were either irradiated with UV light (366 nm, 8 mW cm^{-2}) or white light (400–700 nm, 500 Lumen) for 1 min. Mass transfer rates of caffeine were measured under UV irradiation (366 nm, 8 mW cm^{-2}) and at daylight. After filling the receptor chamber with water, the membrane was fixed in the diffusion cell. The donor chamber was charged with a caffeine solution (93 mM, 3.0 mL). Samples (200 μL) were collected from the receptor part of the cell, typically after 1, 15, 30, 45 min and 1, 1.5, 2, 2.5, 3, 4, 5, 6, 7, 8, 9, 10, 11, 12 h. The caffeine concentrations in these aliquots were determined by measuring its UV absorptions at 293 nm (calibration curve: $c_{aff} = (0.9068x + 0.0212)$ mmol L^{-1}, x: measured absorption). The permeability of a membrane at a given caffeine concentration is proportional to the molecular flux F of aqueous caffeine through the membrane, calculated according to

$$F = n/(At) \quad (2)$$

where n (g) represents the amount of material that diffuses through a membrane, A (cm^2) is the examined section per time t (s). All membranes were stored in water to pre-condition the membranes prior to the permeability measurements.

Electrochemical data was obtained on a CH Instruments 900B potentiostat using platinum mesh and silver wire as the counter and reference electrodes; membrane coated FTO, or a Pt disk electrode were used as the working electrodes for the membrane and solution samples respectively. In the case of the membrane samples, ITO coated glass slides from Sigma-Aldrich (resistivity 8–12 Ω sq^{-1}) were functionalized with acrylated silane. The substrates were cleaned in an argon/oxygen (gas flow 16 : 4 sccm) plasma chamber at 80 W for 15 min under vacuum (self-built asymmetric reactor chamber with a circular gas showerhead powered by a Dressler). Surfaces were then immersed for 2 h under argon flow at room temperature into a solution of 20% 3-methacryloxypropyl trimethoxysilane in dry toluene. After modification, ITO electrodes were rinsed with toluene and water before being dried in a desiccator over molecular sieves. TP1 and iron(II) chloride were added together in a ratio of 2 : 1 (ligand/metal) in methanol (10 mL) and after one hour the solution was treated with excess ammonium hexafluorophosphate and water (3 mL) to precipitate $[Fe(TP1)_2][PF_6]_2$. The suspension was filtered over Celite and washed with cold methanol (83% yield).

All samples were run in HPLC grade acetonitrile containing 0.1 M $[n\mathrm{Bu_4N}][PF_6]$ as the supporting electrolyte at a scan rate of 0.1 V s^{-1}; all solutions were degassed with argon. Cyclic voltammetry was performed on homoleptic iron(II) complexes (*ca.* 10^{-4} mol dm^{-3}) and on membranes fixed to indium tin oxide (ITO) coated glass slides. Cp_2Fe was added to the electrolyte after each set of scans and run as an internal reference.

Results and discussion

Redox behaviour of TP1 monomer in the presence of Co(II)/Co(III) or Fe(II)/Fe(III) redox pairs

Compound TP1 behaves as typical tpy ligand and forms 2 : 1 complexes with transition metal ions such as iron(II) or cobalt(II) in methanol.[39,40,42] The complex formation leads to intensely purple (Fe^{2+}) or orange (Co^{2+}) coloured solutions. The homopletic complexes $[M^{2+}(TP1)_2][PF_6]_2$ were isolated as purple (Fe^{2+}) and orange (Co^{2+}) solids. The presence of the paramagnetic cobalt(II) ion bound to the TP1 ligand was confirmed by ^{1}H NMR experiments where unusually strongly de-shielded resonances are characteristic of $[Co(tpy)_2]^{2+}$ complexes (Fig. S1†). After oxidation with bromine vapor, all ^{1}H NMR resonances were observable in their "normal" chemical shift region, confirming the formation of the diamagnetic Co(III) complex (Fig. S3b and c†).[42]

The reversibility of the oxidation/reduction reactions of the Co(II)/Co(III) couple in the presence of TP1 ligand is shown by

two redox cycles in Fig. 1. The paramagnetic Co(II) shows a pronounced UV absorption at 400–500 nm which is not present in the yellow Co(III) complex (diamagnetic).

Oxidations were performed by bromine vapour and reductions with ascorbic acid.

A slight change in the optical properties after the first redox cycle may be due to the acidity of the ascorbic acid employed in the Co(III)/Co(II) reduction which affects the dispersion/aggregation of tpy units in solution. It is worth mentioning that the redox switching occurs with relatively mild and biocompatible oxidising and reducing agents. Previous studies have already shown low switching potential (*i.e.* −0.30 V *vs.* SCE for 2,2′-bipyridine with Co(II)/Co(III)) and versatility in the choice of oxidizing and reducing agents when cobalt(II)–tpy complexes are deployed.[43,44] This feature is extremely useful for drug delivery applications, where the main target is to vary the permeability of the membrane without any chemical modification of the loaded drug.

Characterization and redox switch behaviour of APCNs modified with TP1 in the presence of Co(II)/Co(III) or Fe(II)/Fe(III) redox pairs

Mechanically stable films of amphiphilic polymer co-networks were synthesized for use as membranes. Amphiphilic poly(2-hydroxyethyl acrylate)-*co*-poly(dimethylsiloxane) (PHEA-*co*-PDMS) co-networks were chosen as substrate due to their inherent mechanical stability, functionalization versatility, the wide composition range in which the nanophase separation occurs and straightforward synthesis.[19,45–48] Such networks are synthesized *via* white-light initiated radical copolymerization of α,ω-dimethacryloxypropyl-terminated PDMS with the hydrophobic trimethylsilylated HEA to prevent macrophase separation prior to polymerization.[19] The silyl protecting groups are then removed using a THF/H_2O 50/50 vol% solution to transform the TMS-protected acrylate co-network segments into the respective hydrophilic PHEA segments. This de-protection step

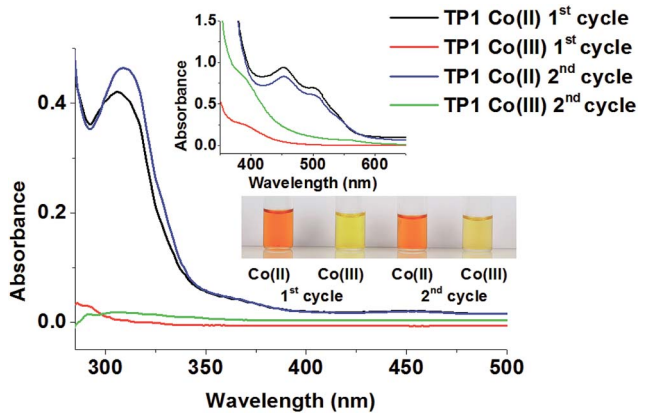

Fig. 1 Optical changes recorded by UV-Vis in CH_3OH during two consecutive redox cycles of TP1 (0.1 wt%) and Co(II)/Co(III) complex ([$CoCl_2$] = 16.8 mM). Bromine vapour was used as oxidant whereas ascorbic acid (0.1 M) was the reducing agent. In the inset, double concentrations of $CoCl_2$ and TP1 were employed.

was followed *via* the appearance of a band in the IR spectrum at 3400 cm^{-1} corresponding to the free –OH group.

Co-polymerizations with TP1 and/or SP monomers were achieved by thoroughly mixing together with HEA prior to initiating the reaction (Scheme 3). We determined *via* absorbance calibration at 556 nm after complexation with Fe(II) that about 94% of the total mass of TP1 added to the solution was co-polymerized in the membrane (Fig. S4†). The analysis of the membrane by XPS confirmed the presence of terpyridine with a weak peak corresponding to 0.46% of N 1s in the organic matrix (400 eV) (Table S1†).

The inclusion of tpy metal-binding domains in the APCNs cause a slight increase of the overall swelling of the matrix in *n*-hexane and an opposite trend with swelling in water, probably due to the higher hydrophobicity of the membrane once the hydroxyl groups are replaced by tpy domains (Fig. S6B†). As a result, also the contact angle values increases from 82° up to 105° once the amphiphilic co-network is functionalized with 0.4 wt% of TP1 (Fig. S8b†).

Inclusion of TP1 in the polymer network (*i.e.* 0.4 wt%) did not alter the overall behaviour of the APCN membrane, as at increasing PHEA/PDMS ratios (*i.e.* by increasing the hydrophilic phase), the swelling in water slightly increase whereas the opposite trend is observed for swelling in hexane (Fig. S5†).

This feature has already been observed in previous pristine APCNs membrane[19,45] Both swellings are independent but are rather low compared to hydrogels because the two covalently linked phases restricted each other. Therefore, the incorporation of tpy does not affect the inherent properties of APCNs.

The TP1 functionalization degree did not affect the overall swelling of the matrix, although the permeability values of the modified APCN membrane at increasing content of TP1 from 0 to 3.2 wt% shows a minimum with 0.4 wt% TP1 (Fig. S6a†).

This effect might be the result of two different phenomena: on one side, at lower TP1 content, hydrophobic interactions between the tpy domains might become prevalent and the consequent increase in the network interactions could contribute to a reduction of the nanochannels size and in the permeability. On the other hand, the increase of free volume occurring by weaker binding between the acrylic phases contributes to an increase in permeability.

The formation of metal cross-linking occurring between the tpy moieties present in the functionalized APCNs was tested by the addition of $CoCl_2$ and $FeCl_2$ (complexation studies of the single TP1 monomer can be found in the ESI†).

The complexation of Co^{2+} to polymer-bound TP1 sites was studied by the UV-Vis absorbance at 455 nm as function of the TP1 concentration (Fig. 2A). We found a continuous increase of the absorbance between 0.2 and 3.2 wt% of TP1 in the presence of sufficient amounts of cobalt, whereas the reference spectrum of $CoCl_2$ solutions showed no absorbance at this wavelength. Furthermore, we followed the kinetics of iron(II) to polymer bound TP1 by monitoring the strong absorbance at 559 nm (ref. 40) (Fig. 2B). We observe no further increase of the intensity of this band after 8 hours indicating that all present TP1 sites were fully complexed with iron.

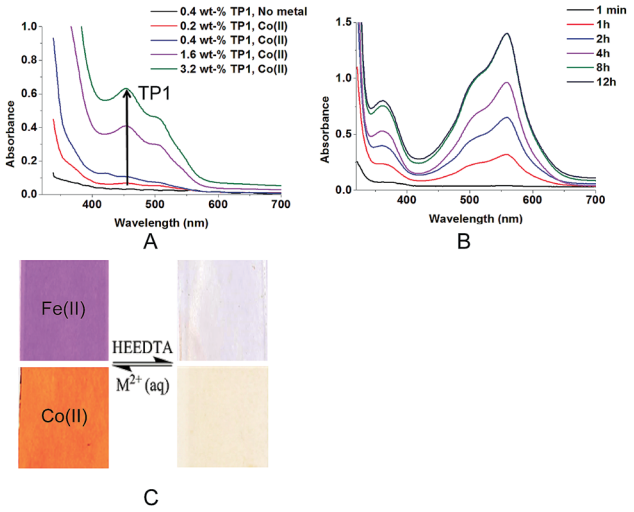

Fig. 2 UV-Vis spectra of membranes with different TP1 contents (0.2–3.2 wt%) after two days reaction with 10 g L^{-1} $CoCl_2$ (A) and complexation kinetics of 0.4 wt% TP1 functionalized APCNs monitored by UV-Vis measurements at a concentration of 5 g L^{-1} iron(II) chloride in aqueous solutions (B). Change of colour of the APCN membranes is associated with both Co(II)/Co(III) and Fe(II)/Fe(III) systems when complexation occurs (C).

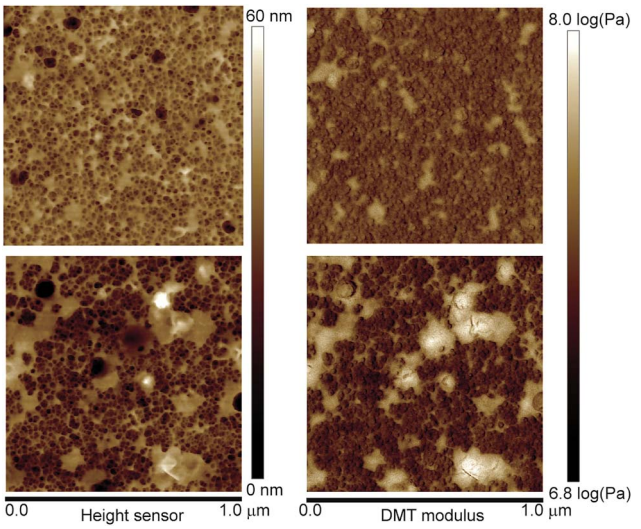

Fig. 3 Variation of height sensor (left) and DMT modulus (right) of TP1 (0.4 wt%) functionalized APCNs as measured by AFM before (top) and after (bottom) exposure to 10 g L^{-1} $CoCl_2$.

In the case of a methacrylate polymer functionalized with tpy units, it has previously been shown that the complexation kinetics of Cu(II) ions, observed as an increase in solution viscosity, went to completion within a period of two days.[49] In our case, the complexation reaction reached equilibrium after 8 h. The faster kinetic of our Fe(II)–tpy system might be related to the overall higher surface area (*i.e.* presence of nanochannels) of APCN compared to the previously studied methacrylate polymer.

It is important to notice how the supramolecular cross-linking density, in turn related to the swelling and permeability, can be tuned by the functionalization degree of terpyridine in the membrane, the concentration of metal ion in solution and the complexation time.

The complexation between tpy and iron(II) was previously demonstrated to be reversible upon addition of the hydroxyethyl(ethylenediaminetriacetic acid) (HEEDTA), a competing metal chelator.[35,50,51] In this study, the reversible complexation/decomplexation of the membranes with cobalt(II) and iron(II) was observed by the colour switch upon treatment with HEEDTA (Fig. 2C). We expected two opposite structural responses of the membrane upon complexation with a metal. The first one is an increase in the swelling capacity due to increasing number of ionic groups in hydrogel.[52] The second mechanism is an intermolecular crosslinking of the PHEA phase.[43,53] We determined the degree of crosslinking of membranes with 0.4 wt% of TP1 without metal and after complexation in cobalt chloride, by PeakForce QNM images (Fig. 3). Peak force atomic force microscopy (AFM) height maps and DMT modulus maps of the amphiphilic co-network shows, in the absence of any complexation, a nanophase separation even when PHEA is functionalized with TP1 (Fig. 3).

The bright phase is assumed to be PHEA whereas the dark phase is assumed to correlate with PDMS.[19,45] It is important to notice how the height maps and the DMT modulus maps show specular profiles. Therefore, this difference between the two phases at constant force might be a consequence of the lower Young's modulus for the PHEA phase.

Upon complexation with cobalt(II) chloride, the nanophase structures collapse to form phase aggregates as a result of the cross-linking occurring in the PHEA phase. This aggregation is registered also by mapping the DMT modulus of the network (right in Fig. 3), where an increased stiffness of the membrane caused by a tighter network induce an increase in the DMT modulus mainly in the PHEA phase. As our previous study has already shown,[19] also adhesion maps confirm the interconnected structure of the PHEA domains, obtaining higher values of adhesion for the PHEA phase as compared to the PDMS phase.

Influence of redox cycles on optical, morphological and permeability properties of APCNs

In the first section, we have shown the fully reversible redox switching between Co(II) and Co(III) in the presence of the TP1 monomer (Fig. 1). Once TP1 is covalently functionalized in the APCN membrane, a similar switch would result in two different permeability states. This is indeed observed by performing two redox cycles for the TP1 functionalized co-network (Fig. 4). Oxidation occurred after submerging the membrane in a hydrogen peroxide solution. It is reflected by a change in colour to yellow, a decrease of the absorbance at 455 nm and an increase in the permeability.

The increase in permeability upon oxidation from Co(II) to Co(III) of the redox responsive membrane is about 10% and the illustrated two redox cycles show a substantial repeatability (within the standard deviation error) of the two different permeability states.

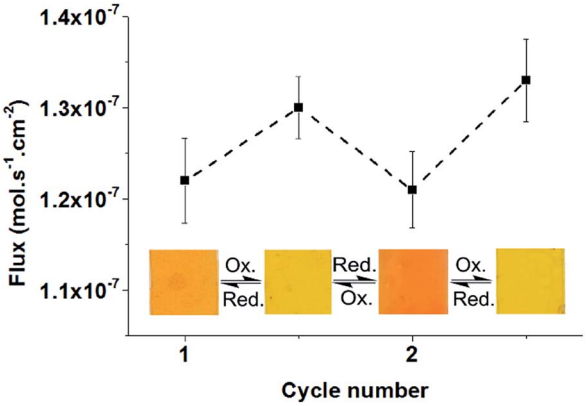

Fig. 4 Reversibility of redox response: permeability of Co(II) loaded membranes containing 1.6 wt% TP1. The flux is calculated based on the slope of the absorbance of caffeine as a function of time (Franz diffusion cell).

The effect on the permeability is associated with an 8% increase in the swelling in water in the presence of the higher oxidation state of metal ion due to an increase in the overall polarity of the network (Fig. S9†). The reversibility of the membrane redox responsive properties are demonstrated by a return to the original cobalt(II) state upon chemical reduction with ascorbic acid.

In order to study the Fe/TP1 monomer electrochemical response, an iron(II) homoleptic complex $[Fe(TP1)_2]^{2+}$ was prepared and measured by solution phase electrochemistry in acetonitrile (Fig. 5A) the cyclic voltammogram showed, one reversible metal-centered oxidation at $E_{1/2} = +0.59$ V, two reversible ligand-centred reductions at $E_{1/2} = -1.74$ and -1.92 V (*vs.* Fc/Fc^+) corresponding to $TP1/TP1^-$ and $TP1^-/TP1^{2-}$ redox couples, and some irreversible reductions at higher negative potentials (-2.40 V) that were assumed to be $TP1^{2-}/TP1^{3-}$ and reductions on the alkene groups.[54,55]

The values for the isolated complex $[Fe(TP1)_2][PF_6]_2$ were then compared with the cyclic voltammogram obtained from an iron complexed membrane with 1.6 wt% of TP1 coated on ITO-coated glass slides (Fig. 5B). The results showed a reversible oxidation at $E_{1/2} = +0.66$ V after stabilization of the system. If compared with the metal-centered oxidation of the iron complex of the TP1 monomer, the $E_{1/2}$ shows similar values as expected.

Thus it can be stated that the inclusion of TP1 in the membrane does not affect the redox behavior of the Fe(II)/Fe(III) transition.

Influence of redox and light switches on permeability, swelling and surface properties of APCNs

The light-responsive properties of SP-functionalized APCNs were previously characterized by UV-Vis and permeability measurements.[19] Under UV light, the isomerization from SP to the merocyanine (MC) zwitteronic form with an extended conjugated π-electron system resulted in an increase of up to 50% of the permeability and the development of a strong absorption band around 545 nm. This significant change in

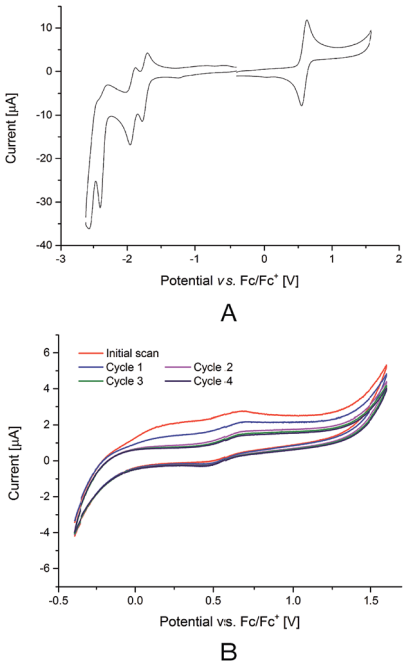

Fig. 5 Cyclic voltammograms of homoleptic iron complex of TP1 (A) and APCN membranes functionalized with 1.6 wt% TP1, complexed with $FeCl_2$ and coated on double layer ITO/glass (B); MeCN solutions containing 0.1 M $[nBu_4N][PF_6]$ as the supporting electrolyte (*vs.* Fc/Fc^+; scan rate = 0.1 V s^{-1}).

permeability due to an increase in polarity proved beneficial for implementing a membrane gating or drug delivery system.[19,22]

The switch in optical absorbance of APCNs membranes functionalized with 0.4 wt% TP1 and 1.0 wt% SP units was tested in the de-complexed state and when Fe(II) and Co(II) were incorporated in the network (Fig. S7†). This study has been performed to understand whether the inclusion of TP1 in the network affects the SP/MC light switch.

The effect of UV light on all the absorption spectra was characterized by the development of an intense band at a wavelength of about 545 nm. The intensity of the band at 545 nm determined from the difference between the absorbance after 1 min white light and the one after 1 min UV light quantifies the influence of the metal on the merocyanine UV-Vis spectrum. Although a slight hypsochromic shift was observed due to change in the polarity and in the degree of flexibility of the SP inside the membrane, the spiropyran-merocyanine isomerization occurs in all samples tested.

Although the functionalization of APCNs with TP1 has shown a 30% increase in the contact angle, SP-modified membranes did not reveal any significant differences compared to the pristine ones (Fig. S8†). Once both SP and TP1 are present in the co-network, swelling and contact angle values are within the range observed in the presence of a single switching functionality.

In addition, an increase in water swelling as well as a decrease in contact angle and hexane swelling was observed on moving from the de-complexed to the complexed stage for SP and TP1 functionalized membranes (Fig. S9†). This is probably

induced by the overall increase in the network polarity as a consequence of the metal ion inclusion.

A higher difference in flux was observed between de-complexed stage and the cobalt(II) treated material under UV light (6% under white light and 16% under UV light). No change in contact angle occurred, suggesting that structural rearrangements occur in the bulk or within one phase of the APCN.

By comparing the effect of UV light with and without cobalt, it is clear that the increase in polarity is much higher in the presence of the metal ion, especially with Co(III). This change is reflected in a slight increase in the swelling degree in water, a noticeable difference in contact angle and a larger difference in permeability between UV and white light. Such divergence in permeability might be explained by stabilization of the merocyanine form which causes a shift in the spiropyran/merocyanine (MC) equilibrium.[56,57]

Hence, membranes containing both TP1 and SP ligands, show that the light, metal and redox state, have synergic effects on the UV-Vis spectrum and permeability.

The reversibility of the isomerization from SP to the MC form in a membrane with 0.4 wt% TP1 and 1 wt% SP complexed to Co(II) was evidenced by a change in colour and the increase in absorption peak of the merocyanine form at 544 nm (Fig. 6A).

The synergic effect of the redox Co(II)/Co(III) couple and the light switch spyropiran/merocyanine showed four different possible states of permeability rates for the SP and TP1 APCNs membrane (Fig. 6B). The difference in permeability between open and closed forms of SP is constant at 45% in the presence of Co(II) or Co(III), whereas an overall increase of 96% in permeability can be observed from State 1 (white light, no metal) to State 6 (UV light, Co(III)). The encapsulation of a light switch in the redox-responsive membrane tremendously increases the permeability range in which the dual-responsive system is able to operate. Previously synthesized spiropyran-modified APCNs have shown only a 50% variation between the SP-APCN and MC-APCN forms.[19] The enhanced control in permeability and the highest range achievable with this matrix allows a finer tuning of the pharmacokinetic effect for drug-delivery applications.

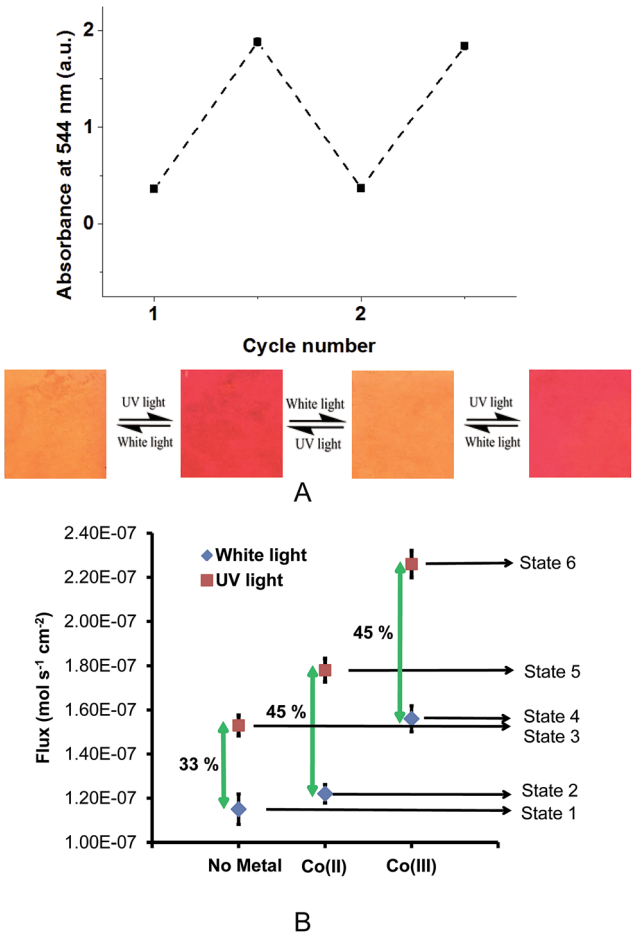

Fig. 6 Reversibility of the white light/UV light switch shown by UV-Vis spectroscopy for 0.4 wt% TP1 and 1 wt% SP functionalized APCNs after complexation with 10 g L^{-1} of $CoCl_2$ for 48 h (aq) (A); four different states of permeabilities for 0.4 wt% TP1 and 1 wt% SP functionalized APCNs in the presence of light and redox switches (B).

Conclusions

In conclusion, we have prepared mechanically-stable multi stimuli-responsive membranes by copolymerizing acrylate-terminated spiropyran and tpy monomers with TMS-protected 2-hydroxyethylacrylate and a methacrylate-terminated poly(dimethylsiloxane) cross-linker. After light-induced copolymerization and deprotection, the system exhibits a nanophase separated amphiphilic co-network structure with variable morphology and hydrophobicity depending on the terpyridine, spiropyran, PHEA and PDMS contents. Complexation of tpy with cobalt(II) or iron(II) in aqueous solution led to a material with a tunable degree of crosslinking. Furthermore, by incorporating these metal ions in the membranes, metal complexes addressable to external stimuli were formed. As a result, we demonstrated the changes in permeability, optical and morphological properties as a response to complexation/de-complexation, redox conditions and light. Furthermore, all combinations of responsive environment, *i.e.* metal ions/HEEDTA (competitive ligand), oxidative/reductive agents and UV/white light, were shown to induce reversible changes in their optical properties. It was demonstrated that the combination of different stimuli-responsive monomers not only lead to an extension of the single responsive functionalities towards multi-responses, but also to a synergistically increased response in permeability upon two or more stimuli. These metal ion-, redox- and light-responsive membranes showing multiple reversible property variations are thus exceptionally promising for their use in drug-delivery applications.

Acknowledgements

Katrin Schöller is grateful for a Marie Curie postdoctoral fellowship (FP7) from 2012–2014. The authors gratefully acknowledge the support of Max Aeberhard, Lea Oberhänsli, Karl Kehl and Patrick Rupper.

Notes and references

1 G. Erdodi and J. P. Kennedy, *Prog. Polym. Sci.*, 2006, **31**, 1–18.
2 C.-W. Wang, C. Liu, X.-W. Zhu, Z.-Y. Yang, H.-F. Sun, D.-L. Kong and J. Yang, *J. Polym. Sci., Part A: Polym. Chem.*, 2016, **54**, 407–417.
3 G. Kali, T. K. Georgiou, B. Iván, C. S. Patrickios, E. Loizou, Y. Thomann and J. C. Tiller, *Macromolecules*, 2007, **40**, 2192–2200.
4 C. Lin and I. Gitsov, *Macromolecules*, 2010, **43**, 10017–10030.
5 Y. Sun, J. Maughan, R. Haigh, S. A. Hopkins, P. Wyman, C. Johnson, N. J. Fullwood, J. Ebdon, S. MacNeil and S. Rimmer, *Macromol. Symp.*, 2007, **256**, 137–148.
6 N. Bruns and J. C. Tiller, *Nano Lett.*, 2005, **5**, 45–48.
7 G. Erdodi and J. P. Kennedy, *J. Polym. Sci., Part A: Polym. Chem.*, 2005, **43**, 4965–4971.
8 M. Hanko, N. Bruns, S. Rentmeister, J. C. Tiller and J. Heinze, *Anal. Chem.*, 2006, **78**, 6376–6383.
9 S. K. Jewrajka, G. Erdodi, J. P. Kennedy, D. Ely, G. Dunphy, S. Boehme and F. Popescu, *J. Biomed. Mater. Res., Part A*, 2008, **87**, 69–77.
10 J. Kost and R. Langer, *Adv. Drug Delivery Rev.*, 2012, **64**, 327–341.
11 S. Mura, J. Nicolas and P. Couvreur, *Nat. Mater.*, 2013, **12**, 991–1003.
12 A. Chan, R. P. Orme, R. A. Fricker and P. Roach, *Adv. Drug Delivery Rev.*, 2013, **65**, 497–514.
13 R. Cheng, F. Meng, C. Deng, H.-A. Klok and Z. Zhong, *Biomaterials*, 2013, **34**, 3647–3657.
14 Y. Zhao, in *Smart Light-Responsive Materials*, John Wiley & Sons, Inc., 2008, pp. 215–242.
15 S. Menon, R. Thekkayil, S. Varghese and S. Das, *J. Polym. Sci., Part A: Polym. Chem.*, 2011, **49**, 5063–5073.
16 M. Herder, B. M. Schmidt, L. Grubert, M. Pätzel, J. Schwarz and S. Hecht, *J. Am. Chem. Soc.*, 2015, **137**, 2738–2747.
17 B. Heinz, S. Malkmus, S. Laimgruber, S. Dietrich, C. Schulz, K. Rück-Braun, M. Braun, W. Zinth and P. Gilch, *J. Am. Chem. Soc.*, 2007, **129**, 8577–8584.
18 R. Klajn, *Chem. Soc. Rev.*, 2014, **43**, 148–184.
19 K. Schöller, S. Küpfer, L. Baumann, P. M. Hoyer, D. de Courten, R. M. Rossi, A. Vetushka, M. Wolf, N. Bruns and L. J. Scherer, *Adv. Funct. Mater.*, 2014, **24**, 5194–5201.
20 L. Baumann, D. de Courten, M. Wolf, R. M. Rossi and L. J. Scherer, *ACS Appl. Mater. Interfaces*, 2013, **5**, 5894–5897.
21 L. Baumann, K. Schöller, D. de Courten, D. Marti, M. Frenz, M. Wolf, R. M. Rossi and L. J. Scherer, *RSC Adv.*, 2013, **3**, 23317–23326.
22 A. C. Pauly, K. Schöller, L. Baumann, R. M. Rossi, K. Dustmann, U. Ziener, D. de Courten, M. Wolf, L. F. Boesel and L. J. Scherer, *Sci. Technol. Adv. Mater.*, 2015, **16**, 1–13.
23 F. Meng, W. E. Hennink and Z. Zhong, *Biomaterials*, 2009, **30**, 2180–2198.
24 P. Kuppusamy, H. Li, G. Ilangovan, A. J. Cardounel, J. L. Zweier, K. Yamada, M. C. Krishna and J. B. Mitchell, *Cancer Res.*, 2002, **62**, 307–312.
25 E. Lallana and N. Tirelli, *Macromol. Chem. Phys.*, 2013, **214**, 143–158.
26 M. Huo, J. Yuan, L. Tao and Y. Wei, *Polym. Chem.*, 2014, **5**, 1519–1528.
27 A. Ghoh, S. Banerjee and B. Voit, *Porous Carbons – Hyperbranched Polymers – Polymer Solvation*, 2015, vol. 266.
28 M. Gallei, *Macromol. Chem. Phys.*, 2014, **215**, 699–704.
29 A. K. Miller, Z. Li, K. A. Streletzky, A. M. Jamieson and S. J. Rowan, *Polym. Chem.*, 2012, **3**, 3132–3138.
30 B. Dhara and N. Ballav, *RSC Adv.*, 2013, **3**, 4909.
31 F. Peng, G. Li, X. Liu, S. Wu and Z. Tong, *J. Am. Chem. Soc.*, 2008, **130**, 16166–16167.
32 Z. Sun, F. Lv, L. Cao, L. Liu, Y. Zhang and Z. Lu, *Angew. Chem., Int. Ed.*, 2015, **54**, 7944–7948.
33 M. Tagliazucchi, F. J. Williams and E. J. Calvo, *Chem. Commun.*, 2010, **46**, 9004–9006.
34 A. Kristanti, R. Batchelor, M. Albuszis, J. Yap and P. J. Roth, *Eur. Polym. J.*, 2015, **69**, 499–509.
35 Z. Ge and S. Liu, *Macromol. Rapid Commun.*, 2013, **34**, 922–930.
36 J. F. Gohy, B. G. G. Lohmeijer, S. K. Varshney, B. Decamps, E. Leroy, S. Boileau and U. S. Schubert, *Macromolecules*, 2002, **35**, 9748–9755.
37 M. A. R. Meier, B. G. G. Lohmeijer and U. S. Schubert, *J. Mass Spectrom.*, 2003, **38**, 510–516.
38 A. Gasnier, C. Bucher, J.-C. Moutet, G. Royal, E. Saint-Aman and P. Terech, *Macromol. Symp.*, 2011, **304**, 87–92.
39 S. Köytepe, M. H. Demirel, A. Gültek and T. Seçkin, *Polym. Int.*, 2014, **63**, 778–787.
40 U. Mansfeld, A. Winter, M. D. Hager, R. Hoogenboom, W. Günther and U. S. Schubert, *Polym. Chem.*, 2013, **4**, 113.
41 S. Bode, L. Zedler, F. H. Schacher, B. Dietzek, M. Schmitt, J. Popp, M. D. Hager and U. S. Schubert, *Adv. Mater.*, 2013, **25**, 1634–1638.
42 H. S. Chow, E. C. Constable, C. E. Housecroft, K. J. Kulicke and Y. Tao, *Dalton Trans.*, 2005, 236–237.
43 Y. Chujo, K. Sada and T. Saegusa, *Macromolecules*, 1993, **26**, 6320–6323.
44 T. A. Asoh, H. Yoshitake, Y. Takano and A. Kikuchi, *Macromol. Chem. Phys.*, 2013, **214**, 2534–2539.
45 N. Bruns, J. Scherble, L. Hartmann, R. Thomann, B. Iván, R. Mülhaupt and J. C. Tiller, *Macromolecules*, 2005, **38**, 2431–2438.
46 J. C. Tiller, C. Sprich and L. Hartmann, *J. Controlled Release*, 2005, **103**, 355–367.
47 M. Hanko, N. Bruns, J. C. Tiller and J. Heinze, *Anal. Bioanal. Chem.*, 2006, **386**, 1273–1283.
48 S. Dech, T. Cramer, R. Ladisch, N. Bruns and J. C. Tiller, *Biomacromolecules*, 2011, **12**, 1594–1601.
49 K. J. Calzia and G. N. Tew, *Macromolecules*, 2002, **35**, 6090–6093.
50 H. Hofmeier and U. S. Schubert, *Macromol. Chem. Phys.*, 2003, **204**, 1391–1397.
51 S. Song, Y. Xue, L. Feng, H. Elbatal, P. Wang, C. N. Moorefiel, G. R. Newkome and L. Dai, *Angew. Chem., Int. Ed.*, 2014, **53**, 1415–1419.

52 O. Okay, in *Hydrogel Sensors and Actuators SE - 1*, ed. G. Gerlach and K.-F. Arndt, Springer, Berlin, Heidelberg, 2010, vol. 6, pp. 1–14.
53 S. Bode, R. K. Bose, S. Matthes, M. Ehrhardt, A. Seifert, F. H. Schacher, R. M. Paulus, S. Stumpf, B. Sandmann, J. Vitz, A. Winter, S. Hoeppener, S. J. Garcia, S. Spange, S. van der Zwaag, M. D. Hager and U. S. Schubert, *Polym. Chem.*, 2013, **4**, 4966–4973.
54 S. Seo, J. Lee, S.-Y. Choi and H. Lee, *J. Mater. Chem.*, 2012, **22**, 1868–1875.
55 H. S. Chow, E. C. Constable, C. E. Housecroft, M. Neuburger and S. Schaffner, *Dalton Trans.*, 2006, 2881–2890.
56 J. D. Winkler, C. M. Bowen and V. Michelet, *J. Am. Chem. Soc.*, 1998, **120**, 3237–3242.
57 R. J. Byrne, S. E. Stitzel and D. Diamond, *J. Mater. Chem.*, 2006, **16**, 1332–1337.